# Bose-Einstein Condensation of Microcavity Polaritons in a Trap

R. Balili, *et al.*

*Science* **316**, 1007 (2007);
DOI: 10.1126/science.1140990



Science (print ISSN 0036-8075; online ISSN 1095-9203) is published weekly, except the last week in December, by the American Association for the Advancement of Science, 1200 New York Avenue NW, Washington, DC 20005. 

# Bose-Einstein Condensation of Microcavity Polaritons in a Trap

R. Balili,[1] V. Hartwell,[1] D. Snoke,[1]* L. Pfeiffer,[2] K. West[2]

We have created polaritons in a harmonic potential trap analogous to atoms in optical traps. The trap can be loaded by creating polaritons 50 micrometers from its center that are allowed to drift into the trap. When the density of polaritons exceeds a critical threshold, we observe a number of signatures of Bose-Einstein condensation: spectral and spatial narrowing, a peak at zero momentum in the momentum distribution, first-order coherence, and spontaneous linear polarization of the light emission. The polaritons, which are eigenstates of the light-matter system in a microcavity, remain in the strong coupling regime while going through this dynamical phase transition.

Work in several promising systems has pointed to Bose-Einstein condensation (BEC) of new types of quasiparticles in solids (*1*): a state that can be called a "coherent solid." In such systems, the electronic degrees of freedom of the solid can undergo a phase transition to spontaneous coherence that is analogous in some ways to superconductivity but that also emits coherent radiation.

Several recent experiments (*2*–*5*) have indicated spontaneous coherence in exciton-polariton gases in various two-dimensional (2D) semiconductor microcavity structures. In each of these experiments, a laser was focused on the sample, with polaritons generated at high density at the laser spot. The coherent effects were seen only at the same place where the laser excited the samples and only during the time when the laser was on. Although it was argued with reasonable justification (*1*) that the coherent state created in these experiments had many of the characteristics of a BEC, a basic question has remained: Because the coherent emission occurs only in the region excited by the laser, is it possible that the coherent effects are essentially the same as a nonlinear amplification of the laser itself? Also, because the polaritons were not created in a confining geometry in those experiments, the ground state of the system was poorly defined: The polaritons could freely diffuse away from the excitation region or fall into local minima created by disorder.

We report the demonstration of a spatial trap for the polaritons in the plane of their motion. This trap is well approximated by a harmonic potential at its minimum, allowing confinement of the polaritons at low temperature. Confinement of the particles in a macroscopic trap is known (*6*) to make BEC allowable in two dimensions with a condensate of finite size, similar to a condensate in a 3D trap (*7*). The trap also produces an evaporative cooling effect for the polaritons. Most importantly, we can generate the polaritons with a laser that is focused far from the center of the trap and watch them accumulate in the bottom of the trap where there is no laser excitation. In a trap, the polaritons exhibit the effects associated with spontaneous Bose coherence seen in previous experiments (*2*). The fact that we can see these direct evidences of spontaneous coherence of polaritons in a GaAs-based microcavity structure improves accessibility, because of the growth and fabrication issues for the II-VI semiconductor structures used in previous experiments (*2*).

It is by now well established (*8*) that exciton-polaritons in microcavities act as a gas of weakly interacting bosons with extremely light mass (measured as $7 \times 10^{-5}$ of the vacuum electron mass in our experiments), which implies very high critical temperature for Bose coherent effects. An exciton-polariton is a linear combination of a cavity photon, which has extremely light effective mass in the 2D plane of the cavity, and a quantum-well exciton. Coupling occurs between the photon states and the exciton states because the excitons are generated and decay by a dipole-allowed interband electronic transition. Cavity photons by themselves are essentially noninteracting, but polaritons interact with each other via a short-range interaction due to their exciton component (*9*).

**Trapping polaritons.** Our structures are essentially identical in design with those used in earlier work (*3*, *4*). Three groups of four identical 70 Å quantum wells are located at the antinodes of a cavity photon mode to maximize the coupling of the exciton and photon states. In earlier work (*4*), it was shown that the lasing transition in these structures is distinct from the onset of coherence in the polariton states, because two distinctly different threshold behaviors could be observed. However, those experiments did not use trapping of the excitons, and they also used very different excitation conditions, namely, an intense pulsed laser with photon energy resonant with the lowest polariton states and at a large incident angle.

Exciton-polaritons in these structures can be created by any mechanism that creates electrons and holes in the quantum wells. In the present work, we create free electrons and holes by pumping with a low-intensity circularly polarized beam from a Ti:Sapphire laser, with photon energy that is high above the lowest polariton states (excess energy = 129 meV), at the first reflectivity minimum above the cavity stop band. This process acts as an incoherent source of

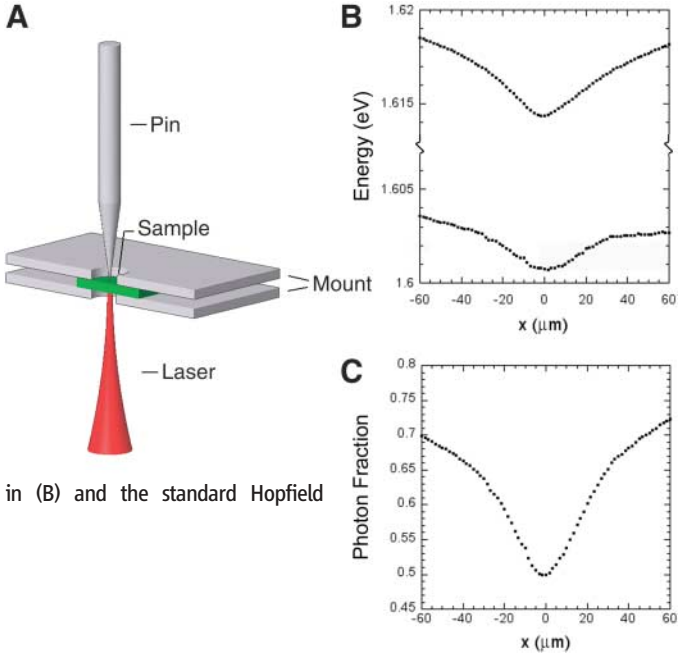


**Fig. 1.** (**A**) Stress geometry for the microcavity structure. (**B**) Upper and lower polariton energies (top and bottom traces, respectively), deduced from photoluminescence and reflectivity spectra at very low excitation density and low lattice temperature ($T$ = 4 K), when a force of 0.975 N on the pin stressor is applied to the sample. (**C**) Photon fraction of the lower polariton branch as a function of position in the trap, calculated from the polariton energies shown in (B) and the standard Hopfield coefficients.

[1]Department of Physics and Astronomy, University of Pittsburgh, 3841 O'Hara Street, Pittsburgh, PA 15260, USA. [2]Bell Labs, Lucent Technologies, 700 Mountain Avenue, Murray Hill, NJ 07974–0636, USA.

*To whom correspondence should be addressed. E-mail: snoke@pitt.edu

polaritons, because the generated electrons and holes must emit many phonons to drop down into the polariton states at the bottom of the band. The pump laser was directed to the sample at an incident angle of $\theta = 17°$; unlike many earlier "magic angle" experiments (*10*–*12*), the angle of the incident beam is not important in our experiments because the photon energy is so far above the polariton states of interest. For all these experiments, the sample was held in helium vapor at temperature $T = 4.2$ K.

Polaritons decay by turning into photons, which exit the cavity. These emitted photons are our primary way of observing the behavior of the polaritons. The in-plane component of the momentum must be conserved in the conversion of polaritons to external photons, which implies that the angle of emission of a detected photon tells us the in-plane momentum of the polariton at the moment of decay. By recording the spectrum of the emitted light as a function of emission angle, we therefore have a complete measurement of the momentum and energy distribution of the polaritons.

The trapping method that we use has been reported earlier (*13*) and is based on a similar method developed for quantum-well excitons (*14*, *15*). In these microcavity structures, the thicknesses of the epitaxial layers vary across the wafer so that the intrinsic detuning of the exciton and cavity photon states varies continuously. For the stress trapping experiments, we choose a piece of the wafer where the cavity is initially negatively detuned, with $\delta \approx -10$ meV ($\delta = E_{cav} - E_{ex}$, where $E_{cav}$ is the cavity photon energy and $E_{ex}$ is the bare exciton energy). As illustrated (Fig. 1A), a force is applied with a rounded-tip pin (tip radius = ~50 μm) on the back side of the substrate, which is ~100 μm thick. The stress shifts the exciton states while the cavity photon energy is left essentially unchanged. Directly under the stressor, the lower polariton branch has an energy minimum (Fig. 1B), which can be well fit by a harmonic potential $U = [1/2]\,\gamma r^2$ (where $r$ is the distance from the center of the trap and $\gamma = 480$ eV/cm$^2$) that corresponds to a quantum level spacing in the harmonic potential of $\hbar\omega_0 = 0.066$ meV (where $\hbar$ is Planck's constant $h$ divided by $2\pi$ and $\omega_0 = \sqrt{\gamma/m}$ is the natural frequency, with effective mass $m$), which is much less than $k_B T$ (where $k_B$ is Boltzmann's constant), so that the continuum approximation for the polariton states in the trap is valid.

The shift of the exciton states with stress also affects the coupling of the exciton states and cavity photon states. In the center of the trap, the cavity photon states and the exciton states are strongly coupled; however, far from the center, the lowest polariton states are almost purely photon-like. Figure 1C shows the photon fraction of the lower polariton branch, deduced from the data of Fig. 1B by means of the standard Hopfield coefficients (*8*). This means that the trap also causes evaporative cooling, because the lifetime of the polaritons at high energy (far from the center) is shorter than the lifetime of those at the energy minimum (in the center). Of course, this effect will work only if the polaritons have diffusion lengths long enough to move through the whole trap. This is the case in our experiments, where in some cases the polaritons move more than 50 μm. In principle, this effect can be increased by the use of larger stress to positively detune the cavity at the center of the trap so that the polaritons are more than 50% exciton-like at the center and become completely photon-like far from the center.

Figure 2 shows a series of images in which the position of the laser spot that creates the polaritons is scanned across the well. The vertical axis of this figure indicates the energy of the polaritons, whereas the horizontal axis gives the spatial position in the plane of their motion. When created by the laser on one side, the polaritons flow down into the trap; when created by the laser on the other side, they flow in the opposite direction into the trap. For these experiments, the laser was quasi–continuous wave (cw), with a 2.4% duty cycle at 1 kHz. The low duty cycle turns out to be essential to see long-range motion of the polaritons, because it reduces the overall heating of the sample; heating of the lattice leads to a very low diffusion constant for the polaritons.

**Signatures of condensation.** Under these conditions, we observe several signatures of spontaneous coherence of polaritons. We observe a critical excitation density threshold for nonlinear gain (Fig. 3A), which is similar to that observed under a wide variety of conditions for polaritons in microcavities (*2*, *4*). Below this threshold, the spectral width of the photoluminescence emitted normal to the surface broadens with increasing density; however, at the threshold, the width of the photoluminescence spectrum drops sharply. At the same time, we observe spatial contraction (Fig. 3B) of the polariton cloud by a factor of three, down to the limit of our spatial imaging resolution (8 μm). [Spatial contraction of the polariton cloud is shown in images in the supporting online

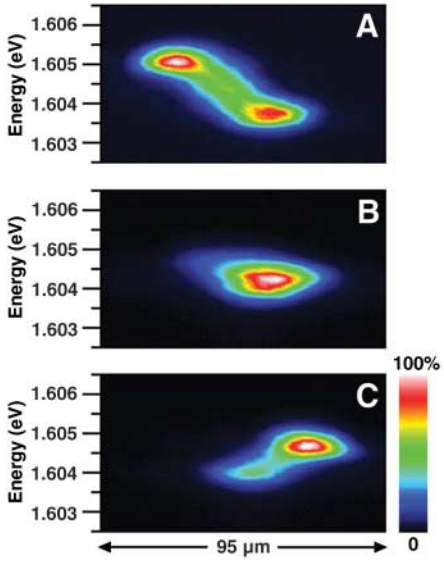


**Fig. 2.** Spatially resolved spectra of the light emission (external angle $\theta = 0 \pm 1.0°$) from polaritons in the microcavity structure for three different positions of the laser. The polaritons are created on the left and flow to the right in (**A**), are created in the trap in (**B**), and are created on the right and flow to the left in (**C**). The average laser power was 2.4 mW for quasi-cw excitation with 2.4% duty cycle at 1 kHz.

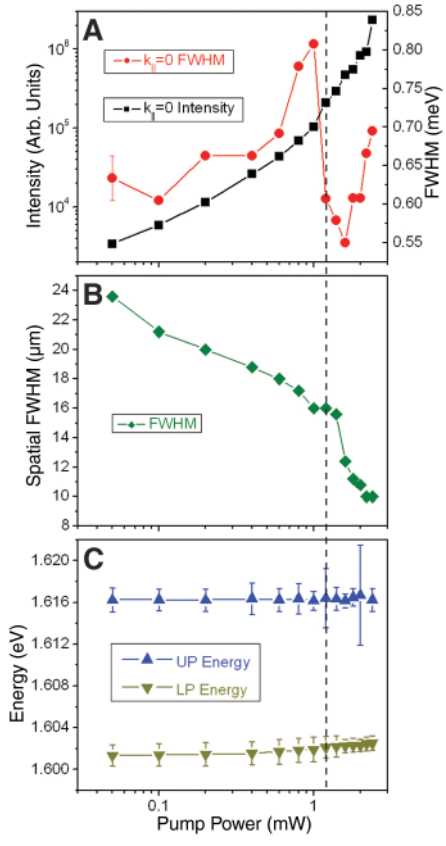


**Fig. 3.** Data for polaritons in the center of the trap when the laser creates the polaritons on the side of the trap, far from the center, similar to the conditions of Fig. 2. (**A**) Black squares indicate total photoluminescence intensity at $k_{||} = 0$ (external angle $\theta = 0 \pm 1.0°$) as a function of average excitation power, for quasi-cw excitation with 2.4% duty cycle. Red circles indicate full width at half maximum (FWHM) of the emission spectrum at $k_{||} = 0$ under the same conditions, which was collected from an 8-μm spot in the center of the trap. (**B**) FWHM of the spatial profile of the photoluminescence collected for external angle $\theta = 0 \pm 5.2°$ from the center of the trap under the same conditions as in (A). (**C**) Upper and lower polariton energies deduced from photoluminescence (lower polariton) and reflectivity (upper polariton) under the same conditions as in (A). The vertical dashed line through the three panels is an indicator of the critical threshold. The error bars in (A) represent the instrumental resolution, and the error bars in (C) are the 1σ uncertainty of the best fit to the data.

material (SOM). The spatial profiles are in marked contrast to previous experiments (*2*) that showed a very irregular pattern of the coherent emission, presumably determined by the local disorder potential.] Spatial contraction is also a telltale sign for condensation in a trap because the condensate seeks the ground state of the system, which (in the case of a trapped gas) is a compact state at the bottom of the trap. Below the critical density, in the normal state, the size of the cloud is determined by a steady-state balance of the pumping by the exciting laser and thermal diffusion; above the critical density, the size of the cloud is given by the size of the ground state of the many-particle system. If interactions are neglected, the standard solution of a harmonic oscillator gives a ground-state wave function with extent $a = \sqrt{\hbar/m\omega_0}$, which for our parameters is 3.8 μm. In the presence of particle-particle repulsion, the size of the ground state will expand (*16*), but its size is still expected to be small as compared to the size of the cloud of thermal particles. This is a major difference between experiments with and without traps: In a translationally invariant geometry, a superfluid will flow outward; whereas, in a trap, it will flow inward. Over the whole range of polariton density, the system remains in the strong coupling regime, as evidenced by the relatively small measured shifts of the lower and upper polariton lines (Fig. 3C).

In addition to these effects, a signature for BEC is the momentum distribution of the particles, which can be measured for polaritons by resolving the angular distribution of the photoemission. Figure 4 shows a series of angle-resolved spectra under the same conditions as in Fig. 3, but with the laser aimed at the center of the trap to give a clearer signal (when the laser is aimed at the side of the trap, the emission from the side of the trap overlaps the signal from the center in the angle-resolved data). There is a dramatic narrowing of both the in-plane momentum $k_{\|}$ and energy of the polaritons above the critical threshold, while the blue shift due to interactions of the polaritons remains very low. The contraction in momentum space that is simultaneous with contraction in real space (Fig. 3B) does not contradict the uncertainty principle because both the spatial cloud size and the momentum distribution are determined by thermal scattering when the polariton gas is in the normal state, below the critical density threshold. Therefore, the total uncertainty in the normal state $\Delta k_{\|}\,\Delta x$ (where $\Delta k_{\|}$ is the uncertainty in the in-plane momentum and $\Delta x$ is the uncertainty in the in-plane position) is much larger than unity. The spatial size of the condensate does imply a minimum width of the momentum peak at $k_{\|} = 0$, which is consistent with our data within our spatial and spectral resolution limits.

Figure 4E shows the relative number of polaritons per $k_{\|}$ state deduced from the same data. The photoluminescence intensity data have been converted to an occupation number with the use of the polariton lifetime deduced from the Hopfield coefficient as a function of $k_{\|}$, as in previous works (*2*, *5*). The energy for each $k_{\|}$ is determined by the maximum of the measured spectrum at each $k_{\|}$, in the same way as in (*2*). Far below the critical density threshold, the polariton distribution is completely nonthermal. Just below the critical density threshold, the distribution is well fit by a Maxwell-Boltzmann distribution $N(E_k) \propto e^{-E_k/k_BT}$ [where $E_k$ is the particle energy, and $N(E_k)$ is the number of particles per state at that energy], which corresponds to a straight line on this plot. Above the critical threshold, there is a sharp increase in the number of polaritons near $k_{\|} = 0$.

The high temperature of the Maxwell-Boltzmann fit below the critical density, which is mirrored in the high-energy tails of the higher-density $N(E_k)$, indicates that the polariton gas is not completely thermalized. As shown in recent theoretical works (*17*–*19*), the lack of complete equilibrium does not prevent the polariton gas from undergoing a phase transition to spontaneous coherence. The buildup of the particles at $k_{\|} = 0$ is truly an effect of the Bose statistics, but the entire range of energy cannot be fit to an equilibrium Bose-Einstein distribution because the high–kinetic energy particles ($E_k$ > ~1.5 meV) are constantly heated by hot polaritons generated by the laser. This is also true of the occupation-number data of (*2*). Steady-state quasiequilibrium theory (*17*–*19*) predicts a bimodal distribution function $N(E_k)$ [with a peak at $k_{\|} = 0$ like that seen in Fig. 4E, which corresponds to a condensate] even when the system is not in complete equilibrium.

Similar to (*2*), we also see spontaneous linear polarization above the critical density threshold (Fig. 5). Below the threshold, the light emission is essentially unpolarized, which is not surprising because the pump light is circularly polarized and the generated carriers must emit numerous phonons. Above the critical threshold, the light becomes linearly polarized. We checked that this polarization is not related to the excitation polarization or to the detection system by rotating the sample relative to the system. We found that the linear polarization follows the sample orientation and is nearly aligned with the [110] axis of the crystal, as in the CdTe experiments (*2*). The polarization angle also appears to depend weakly on the applied stress. Linear polarization has been predicted (*20*) to be a direct result of spontaneous symmetry breaking in the polariton condensate system; more recent theoretical work has shown that pinning along a crystal symmetry direction is expected (*21*). In general, when there is a condensate, any small term in the Hamiltonian that breaks the degeneracy of the ground state will cause the condensate to jump into the lowest energy state.

**Direct measure of coherence onset.** Under slightly different conditions, we can also see direct evidence of coherence in the first-order correlation of the photoluminescence, which is also seen in the work in CdTe structures (*2*). For



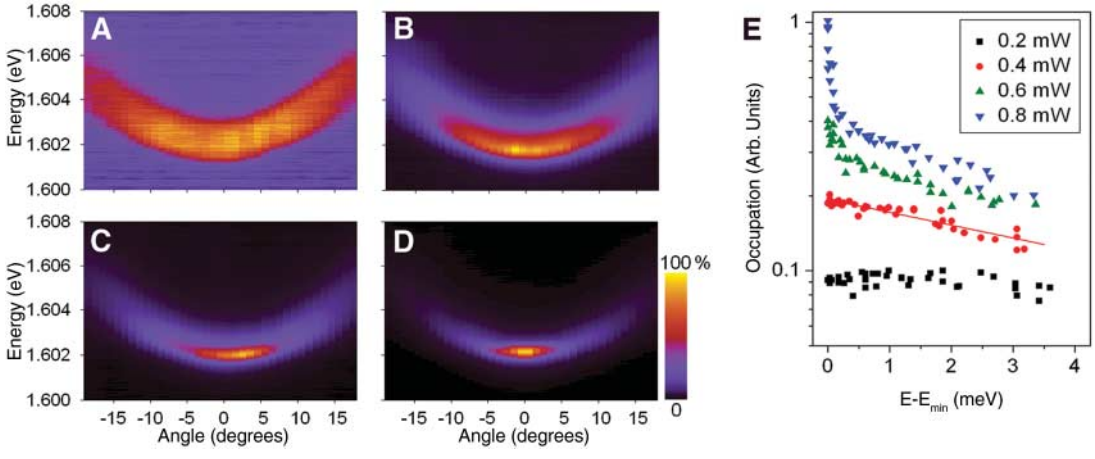


**Fig. 4.** Momentum distribution of the polaritons as measured by angle-resolved photoluminescence intensity for four different powers (under the same conditions as in Fig. 3, but with the laser aimed at the center of the trap). Angle-resolved spectra for (**A**) 0.05-mW pump power (far below the threshold density), (**B**) 0.4-mW pump power (just below the threshold), (**C**) 0.6-mW pump power (at the threshold), and (**D**) 0.8-mW pump power (above the threshold). The false-color scale is linear, with yellow and black indicating high and low values, respectively. (**E**) Number of polaritons per $k$ state, deduced from the data of (A) to (D). The straight line is a fit to a Maxwell-Boltzmann distribution with $T$ = 97 K. $E - E_{min}$ is the peak energy of the luminescence at each angle, relative to the minimum energy (at $k_{\|} = 0$).

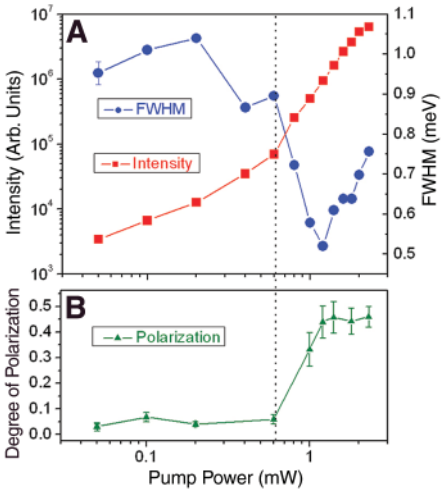


**Fig. 5.** (**A**) Red squares indicate total photoluminescence intensity at $k_{||} = 0$ (external angle $\theta = 0 \pm 1.0°$) as a function of average excitation power, for the same conditions as in Fig. 4. Blue circles indicate FWHM of the emission spectrum at $k_{||} = 0$ under the same conditions, collected from an 8-μm spot in the center of the trap. (**B**) Degree of polarization $[(I_{max} - I_{min})/(I_{max} + I_{min})]$ under the same conditions as in (A).The vertical dashed line is an indicator of the critical threshold. The error bars in (A) represent the instrumental resolution, and the error bars in (B) are the 1σ uncertainty of the best fit to the data.

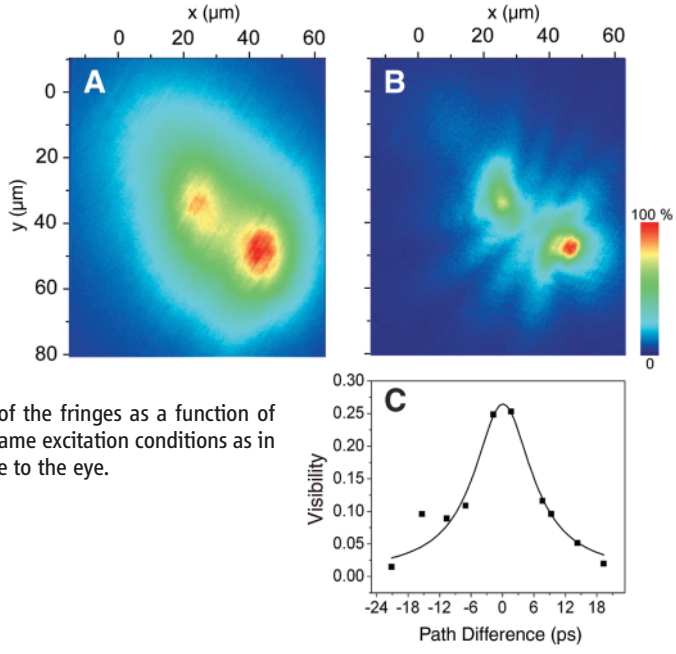


**Fig. 6.** False-color interference pattern created by sending the light emission through a slightly misaligned Michelson interferometer, with the cw pump laser aimed at the center of the trap. Laser power is shown below and above threshold in (**A**) and (**B**), respectively; cw average power is 37 mW in (A) and 73 mW in (B). Total time delay of one path relative to the other was 1.56 ps. (**C**) Visibility of the fringes as a function of path difference under the same excitation conditions as in (B). The solid line is a guide to the eye.

these measurements, we used a cw laser in order to get the maximum luminescence intensity from the sample. The average power of the laser is much higher than in the low-duty-cycle experiments discussed above, and the diffusion constant is much lower than in the low-duty-cycle experiments. However, when the laser is aimed at the center of the trap, we see essentially the same behavior—spectral narrowing, beamlike emission in a narrow range of angle corresponding to polaritons with $k_{||} \cong 0$, and spontaneous linear polarization—as that seen in the experiments with low duty cycle for the pump laser.

Figure 6 shows images produced by sending the spatially resolved photoluminescence through two arms of a Michelson interferometer, when the interferometer is slightly misaligned to create a double image [in which the left side of the image from one arm overlaps with the right side of the image from the other arm (single images of the spot under these conditions are shown in the SOM)]. In this way, we detect the spatial correlation across the length of the polariton cloud, including the low-density tail, which extends 20 μm from the center. Below the critical excitation density threshold, we cannot see any interference fringes for any path difference of the two arms of the interferometer (Fig. 6A). Above the critical density, fringes appear (Fig. 6B). Figure 6C shows the visibility of the fringes, $(I_{max} - I_{min})/(I_{max} + I_{min})$, where $I_{max}$ and $I_{min}$ are the maximum and minimum intensity, respectively, as the path length is varied under the same excitation conditions as in panel B. The visibility is never 100%, which is consistent with recent theoretical predictions (*22*) that the condensate fraction of the polariton gas should be less than 50%. The coherence time increases from less than 1 ps below the critical threshold to 8 to 10 ps above the critical threshold, which is longer than the nominal lifetime of the polaritons in these structures of around 4 ps (*4*).

**Concluding remarks.** The dramatic transition of the system to a linearly polarized, compact, coherent, beamlike light source is consistent so far with the picture of quasiequilibrium BEC of exciton-polaritons. The ability to trap the polaritons allows us to observe many of these effects under conditions when the polaritons are confined in a region far from the laser generation point.

Although it may be hard to visualize polaritons, and although their lifetime is short, this system has all of the same essential features as those of atoms in traps. The polaritons act as a gas, moving through the semiconductor medium, and are trapped in a harmonic potential. The same basic theory of condensates and spontaneous coherence underlies both systems. In this case, the differences are that the system is truly two-dimensional and is in a quasiequilibrium steady state, with an incoherent pump.

### References and Notes


1. D. Snoke, *Nature* **443**, 403 (2006).
2. J. Kasprzak *et al.*, *Nature* **443**, 409 (2006).
3. H. Deng, G. Weihs, C. Santori, J. Bloch, Y. Yamamoto, *Science* **298**, 199 (2002).
4. H. Deng, G. Weihs, D. W. Snoke, J. Bloch, Y. Yamamoto, *Proc. Natl. Acad. Sci. U.S.A.* **100**, 15318 (2003).
5. H. Deng *et al.*, *Phys. Rev. Lett.* **97**, 146402 (2006).
6. P. Noziéres, in *Bose-Einstein Condensation*, A. Griffin, D. W. Snoke, S. Stringari, Eds. (Cambridge Univ. Press, Cambridge, 1995), p. 15.
7. L. Pitaevskiĭ, S. Stringari, *Bose-Einstein Condensation* (Clarendon, Oxford, 2003).
8. A. Kavokin, G. Malpeuch, *Cavity Polaritons* (Elsevier, Amsterdam, 2003).
9. D. Porras, C. Ciuti, J. J. Baumberg, C. Tejedor, *Phys. Rev. B* **66**, 085304 (2002).
10. R. M. Stevenson *et al.*, *Phys. Rev. Lett.* **85**, 3680 (2000).
11. S. Kundermann *et al.*, *Phys. Rev. Lett.* **91**, 107402 (2003).
12. A. Huynh *et al.*, *Phys. Rev. Lett.* **90**, 106401 (2003).
13. R. Balili, D. W. Snoke, L. Pfeiffer, K. West, *Appl. Phys. Lett.* **88**, 031110 (2006).
14. V. Negoita, D. W. Snoke, K. Eberl, *Appl. Phys. Lett.* **75**, 2059 (1999).
15. Z. Vörös, D. W. Snoke, L. Pfeiffer, K. West, *Phys. Rev. Lett.* **97**, 016803 (2006).
16. V. V. Goldman, I. F. Silvera, A. J. Leggett, *Phys. Rev. B* **24**, 2870 (1981).
17. M. H. Szymańska, J. Keeling, P. N. Littlewood, *Phys. Rev. Lett.* **96**, 230602 (2006).
18. D. Sarchi, V. Savona, *Phys. Status Solidi B* **243**, 2317 (2006).
19. T. D. Doan, H. T. Cao, D. B. Tran Thoai, H. Haug, *Solid State Commun.*, in press.
20. F. P. Laussy, I. A. Shelykh, G. Malpuech, A. Kavokin, *Phys. Rev. B* **73**, 035315 (2006).
21. G. Malpuech, M. M. Glazov, I. A. Shelykh, P. Bigenwald, K. V. Kavokin, *Appl. Phys. Lett.* **88**, 111118 (2006).
22. D. Sarchi, V. Savona, *Solid State Commun.*, in press; preprint available at http://arxiv.org/abs/cond-mat/0603106.


23. We thank A. Heberle, H. Deng, G, Weihs, and Y. Yamamoto for invaluable assistance, discussions, and comments, and C. Yang for assistance in some measurements. This material is based on work supported by NSF (grant number 0404912) and by the Defense Advanced Research Projects Agency under the U.S. Army Research Office (contract number W911NF-04-1-0075).


### Supporting Online Material

www.sciencemag.org/cgi/content/full/316/5827/1007/DC1
SOM Text
Figs. S1 to S3
Movie S1

7 February 2007; accepted 28 March 2007
10.1126/science.1140990